Radiation Physics and Chemistry 205 (2023) 110733

Contents lists available at ScienceDirect

Radiation Physics and Chemistry

journal homepage: www.elsevier.com/locate/radphyschem

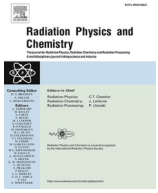

FLASH irradiation does not induce lipid peroxidation in lipids micelles and liposomes

Pascal Froidevaux [a,*], Veljko Grilj [a], Claude Bailat [a], Walter Reiner Geyer [a], François Bochud [a], Marie-Catherine Vozenin [b,**]

[a] Institute of Radiation Physics, Lausanne University Hospital and University of Lausanne, Lausanne, Switzerland
[b] Laboratory of Radio-oncology, Service of Radiation Oncology, Department of Oncology, Lausanne University Hospital and University of Lausanne, Switzerland

ARTICLE INFO

Keywords:
FLASH-radiotherapy
Lipid peroxidation
Ferroptosis
Dose rate
Oxygen
Reactive oxygen species

ABSTRACT

FLASH radiotherapy (FLASH-RT) enables the delivery of ultra-high dose rate (UHDR) radiation to a tumor, increasing the mean dose rate from 0.1 Gy· $s^{-1}$of conventional radiotherapy (CONV-RT) to 100 Gy· $s^{-1}$and above. Animal models have demonstrated that FLASH-RT preserves healthy tissues while yielding similar tumor growth delay as conventional irradiation. Despite the promise of FLASH-RT, the physico-chemical and biological mechanisms underlying the FLASH effect are still under investigation. Two mutually non-exclusive hypothesis have been proposed that could explain the FLASH effect: 1) a reduction in radical diffusion due to a higher recombination rate of primary radicals and, 2) a reduction in tissue oxygenation levels able to alter downstream responses to FLASH-RT. In this respect, lipid peroxidation is a chemical reaction consuming oxygen, which might be involved in the FLASH effect. Here we used linoleic acid micelles and phosphatidylcholine (PC) liposomes as a proxy for cell membrane to investigate the lipid peroxidation yield after irradiation with electrons in FLASH and CONV modalities. With this system, we measured significant differences in concentrations of lipid peroxidation endproducts between both modalities of irradiation. The lipid micelles and PC liposomes exhibited enhanced and linear dose-dependent levels of lipid peroxidation with CONV, while FLASH did not induce lipid peroxidation. Lowering the oxygen content from 21 to 4% resulted in a diminution of the lipid peroxidation yield in CONV, but not its complete suppression. The lipid peroxidation yield dropped rapidly when the dose per pulse was increased from 0.008 Gy·$pulse^{-1}$to 10 Gy·$pulse^{-1}$, with no lipid peroxidation occurring above 0.2 Gy·$pulse^{-1}$. Our results are the first to identify the lack of lipid peroxidation after FLASH-RT, and point to lipids as potentially critical target in rationalizing possible mechanisms underlying the FLASH effect across multiple normal tissue sites.

1. Introduction

FLASH radiotherapy (FLASH-RT) is an irradiation modality where the dose is delivered in a very short time, leading to ultra-high dose rates (UHDR) above 100 Gy s^{-1}, typically more than two orders of magnitude higher than the dose rates used in conventional radiotherapy (CONV) (Kacem et al., 2021). Animal studies have revealed that delivering a dose at UHDR can preserve healthy tissues in various organs and species (lung, skin, intestine, brain, hematopoietic system) (Montay-Gruel et al., 2019, 2021; Vozenin et al., 2019). Additional studies carried out in normal tissue have shown reduced DNA damage (Fouillade et al., 2020), apoptosis (Favaudon et al., 2014; Simmons et al., 2019), fibrosis and inflammatory signaling pathways (Montay-Gruel et al., 2019; Favaudon et al., 2014; Simmons et al., 2019; Buonanno et al., 2019). Unexpectedly, the anti-tumor efficacy of FLASH and CONV-RT remains similar at the same dose level (Montay-Gruel et al., 2021; Montay-Gruel et al., 2019; Favaudon et al., 2014; Bourhis et al., 2019). While multiple investigators using different beam modalities have substantiated the benefits of FLASH-RT, the mechanisms underlying this differential effect between normal tissues and tumors are currently unknown. Several physico-chemical hypotheses have been raised, that involve either a reduction in radical diffusion due to a higher recombination rate of primary radicals (Labarbe et al., 2020; Abolfath et al., 2020) and/or transient local oxygen depletion induced by fast oxygen consumption

* Corresponding author. Institute of Radiation Physics, Grand Pré 1, 1007, Lausanne, CH, Switzerland.
** Corresponding author. Laboratory of Radio-oncology, Service of Radiation Oncology, Department of Oncology, Lausanne University Hospital and University of Lausanne, Switzerland.
E-mail address: pascal.froidevaux@chuv.ch (P. Froidevaux).

https://doi.org/10.1016/j.radphyschem.2022.110733
Received 26 September 2022; Received in revised form 15 December 2022; Accepted 16 December 2022
Available online 17 December 2022

produced by UHDR irradiation (Hendry et al., 1982; Weiss et al., 1974; Spitz et al., 2019). In this respect, lipid peroxidation reactions able to consume oxygen warrants further scrutiny as a possible mechanism underlying the FLASH effect (Labarbe et al., 2020; Spitz et al., 2019).

Reactive oxygen species (e.g. hydroxyl and hydroperoxyl radicals) are the main initiators of non-enzymatic lipid peroxidation in PUFAs. Lipid hydroperoxides undergo further oxidative fragmentation reactions forming unsaturated α,β−aldehydes, including 4-hydroxynonenal (4-HNE) and malondialdehyde (MDA). Both of these molecules define classical surrogates for measuring lipid peroxidation in biological systems. Lipid peroxidation of phospholipids in the cellular plasma and organelle membrane or mitochondrial compartment may lead to alteration of cell signaling, cell dysfunction or death(Dixon and Stockwell, 2019). Sensitivity to lipid peroxidation depends on the activation of the GPX4 system, which will reduce lipid hydroperoxides to more benign alcohols and on the activation of the cystine transporter SLC7A11 (Dixon and Stockwell, 2019; Stockwell et al., 2017; Wiernicki et al., 2020). Suppression of GPX4 lead to strong lipid peroxidation, which may result in cell death, in a process referred as ferroptosis. Ferroptosis is a cell death mechanism, which involves Fe^{2+}in the propagation of the lipid peroxidation reaction (Doll et al., 2017; Lang et al., 2019). Exposure to ionizing radiation is known to trigger antagonistic cellular responses, leading to lipid peroxidation and ferroptosis in certain cases(Lang et al., 2019; Lei et al., 2021a,b; Lei et al., 2020; Pearson et al. (2021)reviewed the contribution oflipidoxidation andferroptosis toradiotherapyefficacyand recognized that there would be therapeuticopportunities tolimitradiotherapytoxicity viaferroptosisinhibition.

The effect of ionizing radiations on lipid oxidation has long been known and the most striking result was the observation of the so-called "inverse dose rate effect" which showed a diminishing in the lipid peroxidation yield when the dose rate wasincreased (Mead, 1952).Stark (1991)reviewed the effect ofionizing radiation on lipid membranes and postulated that the inverse dose rate effect was due to the radical termination reaction, which will overcome the propagation reaction due to the high density of peroxyl radicals formed at high dose rate.

In this study, we contrasted the effects of dose rate modulation using CONV and FLASH on the concentration of specific lipid peroxidation endproducts. To this end, we used micelles of linoleic acid (LA) and liposomes of phosphatidylcholine (PC) as a proxy for the cellular membrane. Lipid micelles and liposomes irradiated with FLASH and CONV-RT were then measured for the concentration of malondialdehyde (MDA) and/or lipid hydroperoxides (LOOH) as a surrogate of the lipid peroxidation yield. We determined the MDA concentration as a function of the depth in water and compared it to the percentage depth dose (PDD) curve. Finally, we tested the MDA production as a function of the dose per pulse of the electron beam.

2. Methods

2.1. Chemicals

Crude phosphatidycholine (~60% in PC), sodium dodecylsulfate (SDS), potassium dihydrogenophosphate hexahydrate (KH_2PO_4), thiobarbituric acid (TBA), trichloroacetic acid (TCA), xylenol orange (XO), ammonium iron (II) sulfate hexahydrate (Fe^{2+}), 2,6-Di-tert-butyl-4-methylphenol (BHT), perchloric acid (PCA), 1,1,3,3,tetrametoxypropane (TMP), dimethylformamide (DMF), trimethylamine (Et_3N), chloroform ($CHCl_3$) and methanol (MeOH) were all of analytical grade and purchased from Sigma Aldrich (Switzerland). 5,5-Dimethyl-1-pyrroline N-oxide (DMPO) was purchase from TCI (Belgium) and was of spectroscopic quality for ESR. All products were used as received except for crude phosphatidylcholine. Crude phosphatidylcholine was freshly purified before use from phosphatidylethanolamine (PE, ~30%) and others impurities (mostly free polyunsaturated fatty acids (PUFA) and saturated fatty acid) on SiO_2 chromatography column with elution gradient of MeOH in $CHCl_3$ (10 → 50%) according to Zhang et al., (2003).

2.2. Linoleic acid micelles preparation

200 μl of linoleic acid (13 mM final concentration) were introduced in a 50 ml solution of 0.3% SDS containing 5 mM KH_2PO_4 adjusted to pH 7.4. The suspension was agitated on a laboratory planar shaker (Gerhardt LS 20) during 2 h in the dark, and then kept at 4 °C until used.

2.3. Phosphatidylcholine liposomes preparation

Phosphatidylcholine used in this work was from egg yolk, which is known to contain about 15% of the easily oxidizable linoleic acid. 500 μl of a phosphatidylcholine solution in $CHCl_3$ (120 mg/ml) were evaporated with a rotary evaporator. 2 ml of 5 mM KH_2PO_4 buffer at pH 7.4 were added and the solution was sonicated 30 s and left wetting for 1 h. The solution was diluted to 5 ml with 5 mM KH_2PO_4 buffer and vortexed for homogeneity. Multilamellar large vesicles were transformed to unilamellar small vesicles (∅ 100 nm) using extrusion (Avanti® Mini-Extruder) through a 100 nm polycarbonate membrane (Avanti polar Lipids®). The solution was diluted with the buffer to 15 ml (final PC concentration: 5.2 mM) and vortexed for homogeneity and kept at 4 °C until used. For PC liposomes loaded with LA, a determined volume of LA leading to a final LA concentration of 2 mM was added to the $CHCl_3$ PC solution before evaporation.

2.4. Oxygen content

If not otherwise stated, the experiments were carried out at 21% atm O_2. For experiments at 4% atm O_2, the vials and solutions were equilibrated overnight with N_2 in a hypoxia chamber (Biospherix C-Chamber with Biospherix ProOx C21 controller). Initial oxygen content of the lipid solutions was measured using the OxiLite Pro™ system (Oxford Optronix).

2.5. Irradiation

Irradiations were performed using a prototype 5.5 MeV electron beam linear accelerator Oriatron eRT6 (PMB Alcen), which was commissioned at Lausanne University Hospital (Jaccard et al., 2018). The dosimetric traceability to international standards is a challenge for UHDR radiation, because the established international reference conditions are not yet available. Lately, our group has developed a robust dosimetric methodology to circumvent this hurdle (Jaccard et al., 2017; Petersson et al., 2017). Accordingly, the absorbed dose in FLASH mode was verified offline by passive dosimeters including the GafChromic EBT3 films and alanine pellets, while the absorbed dose in CONV was measured by the Advanced Markus ionization chamber traceable to the Swiss institute of metrology (METAS). In addition, we utilized the online monitoring system based on inductive current transformers in order to insure the reliability of the delivered dose. This system was recently developed and validated by our group (Oesterle et al., 2021; Jorge et al., 2022). The Oriatron eRT6 generates 0.5–4 μs long pulses at frequencies between 5 and 250 Hz. The irradiator is capable of delivering doses of up to 20 Gy in a single pulse resulting in average dose rates (DR_{av}) as high as 10^7 Gy/s. In dose escalation experiments, the beam was operated in two modes, FLASH and CONV, characterized by the set of parameters shown in Table 1. In each mode, the desired dose was applied by adjusting the number of pulses (N_p). The samples were contained in 2.5 ml

Table 1
Beam parameters used for the dose escalation study on LA micelles and PC liposomes samples. The field size is defined for the 95% isodose.

	E [MeV]	Field size [cm]	SSD [mm]	w [μs]	PRF [Hz]	D_p [Gy]	DR_{av} [Gy/s]
FLASH	4.9	3.4	465	1.8	100	5	>540
CONV	6	3.5	600	1	10	0.014	0.14

polypropylene Eppendorf tubes and irradiated inside the water tank of 30 cm × 30 cm x 30 cm size for absolute dosimetry with horizontal beams (PTW, model 41,023). The tubes contained 2.0 ml of the lipid liposomes solution, which allowed for oxygen diffusion from the gas phase. The tubes were centered at an equivalent depth in water of 10 mm. To investigate the lipid peroxidation as a function of the dose per pulse (D_p), the pulse width (w) and the pulse repetition frequency (PRF) were fixed to 1 μs and 10 Hz, respectively, while the source to surface distance (SSD) was varied from 45 cm to 250 cm. In that way, D_p values between 1 Gy and 0.008 Gy were achieved (Table 2). In all cases, samples containing the PC liposomes were exposed to the same total dose of 40 Gy.

2.6. Malonedialdehyde determination by HPLC

20 μl of a 0.5 M BHT solution in DMF were added to the irradiated or non-irradiated (blank) samples to stop the lipid peroxidation and vortexed for homogeneity. One ml was sampled to a 2 ml Eppendorf tube and 1 ml of a 10 mM TBA solution in 7.5% TCA was added and the suspension vortexed 30 s. The Eppendorf tube was centrifuged at 13′000 rnd per minute for 20 min (RCF 12′300). One ml of the supernatant was transferred to a 2.5 ml glass vial and heated at 95 °C during 1 h in a heating block (Fisherbrand Isotemp), leading to the synthesis of the MDA-TBA pink adduct. The MDA-TBA adduct was separated and quantified using HPLC (Thermo scientific UltiMate 3000) on a reverse phase column (Lichrospher® 100 RP 10, 5 μm, n° 528,600) with KH_2PO_4 100 mM/0.2% Et_3N solution in MeOH (6:4 v:v) at pH 6.8 as isocratic eluent and absorbance at 532 nm. Calibration curve was made with TMP at 0.3, 0.6, 1.0, 1.5 and 2.0 μM following hydrolysis and MDA-TBA synthesis. Because lipids already contain a certain amount of autoxidation (MDA and LOOH), MDA concentrations are the results of HPLC determination minus the average value of at least three blank replicates, which were non-irradiated samples.

2.7. Lipid hydroperoxides determination

Lipid hydroperoxides (LOOH) were determined as described by Gay and Gebicki (2003). Briefly, 200 μl of the irradiated (or blank) solution are extracted by 900 μl of a mixture of MeOH/$CHCl_3$ (1:2) and centrifuged. H_2O_2 produced by the irradiation was present in the aqueous phase (not measured) while the organic LOOH were present in the organic phase. 400 μl of the $CHCl_3$ phase was sampled in a 2 ml glass vial and evaporated to dryness under a N_2 flux. 250 μl of $CHCl_3$ (4 mM in BHT), 400 μl of MeOH (4 mM in BHT), 41 μl PCA 2 M, 30 μl of 5 mM XO and 20 μl of 5 mM Fe^{2+} were added. After incubation at room temperature for 1 h, the Fe^{3+}-XO complex absorbance was measured at 560 nm (Thermo Fisher Evolution 200) in 1 cm glass cuvette. The absorbance at 560 nm was directly proportional to the lipid hydroperoxide (LOOH) concentration, after subtraction of the average absorbance of at least three blank replicates, which were non-irradiated samples.

Table 2
Beam parameters used to investigate the lipid peroxidation as a function of the D_p.

SSD [mm]	w [μs]	PRF [Hz]	D_p [Gy]	N_p	DR_{av} [Gy/s]
2500	1	10	0.008	5000	0.08
2000	1	10	0.014	2860	0.14
1750	1	10	0.020	2000	0.2
1450	1	10	0.030	1330	0.3
1300	1	10	0.040	1000	0.4
1170	1	10	0.050	800	0.5
950	1	10	0.080	500	0.8
880	1	10	0.100	400	1
650	1	10	0.200	200	2
450	1	10	1.000	40	10

2.8. Electron spin resonance (ESR) measurements

ESR measurements were carried out using a Bruker EMX Nano (Bruker, Germany). For the comparison of the escape yield of HO· and H· in CONV and FLASH, 2 ml of a 50 mM DMPO solution as spin trap was irradiated at 20 Gy. To compare the absolute number of spins produced by FLASH or CONV irradiation, our EPR cavity was preliminary calibrated with TEMPOL standards, transforming the relative number of spins determined by the apparatus in absolute concentration of spins. The solution was injected 90 s after irradiation with a syringe in the flow-through cell (Bruker E7004543) inserted in the ESR cavity and the ESR spectrum recorded with the following conditions: Centre field: 3444 G, field width: 110 G, scan time: 30 s, number of scan: 3, receiver gain: 40 dB, modulation amplitude: 1 G, attenuation: 10 dB (10 mW microwave power).

2.9. Uncertainties

Uncertainties on MDA concentration were calculated as a propagation of several individual A-type uncertainties given by i) HPLC calibration: 5% ii) dilutions: 2% iii) MDA-TBA synthesis yield: 5% iv) initial LA and PC concentrations: 4%. Considering additional systematic uncertainties (positioning, O_2 level, temperature variations, etc.), an overall uncertainty of at least 10% for MDA and LOOH dosages must be taken into account for every measure. Overall uncertainty on the irradiation dose was ~5%. (k = 2).

3. Results

3.1. Spin-trapping (DMPO) of the hydroxyl radicals produced in FLASH and CONV

Our 5.5 MeV electron beam linear accelerator Oriatron eRT6 (PMB Alcen) is able to deliver conventional and FLASH irradiations. However, the dosimetry in FLASH modality is a challenge. While several methods have been used to do that with our beam (Jaccard et al., 2018; Petersson et al., 2017; Oesterle et al., 2021; Jorge et al., 2022) we used here radical spin trapping with DMPO to reveal that the beam delivered equivalent dose in FLASH and in CONV by determining the number of spins produced during both irradiation. Radiolysis of water produces the hydroxyl radical (HO·) and we trapped this radical early (~10 ns) in the tracks using 50 mM DMPO after CONV and FLASH. Results showed that both irradiation modalities produced the same amount of spin-trapped H· and HO· radicals (Figs. 1 and 2.64 ± 0.2 μM in CONV against 2.76 ± 0.2 μM in FLASH, for 20 Gy). Both spectra showed similar mixing and signal integration of DMPO-OH and DMPO-H. Thus, differences observed in lipid peroxidation yields between both modalities (see below) was not due to a difference in the initial radical yield during radiolysis. Apparently, the FLASH specific effect transpired later on, probably during the radical diffusion phase (μs) after the pulse.

3.2. Lipid peroxidation in dose escalation experiments

We started experiments using eRT6 5.5 MeV electron beam to induce lipid peroxidation through water radiolysis, which produces the very reactive hydroxyl radical (HO·) able to extract allylic hydrogen atoms of PUFA, e.g. the C-11 hydrogen atom on linoleic acid. Primary effect (direct ionization of lipid) might play a role in lipid peroxidation but secondary effect (mostly hydroxyl radicals) is clearly the main peroxidation initiator. Hydroxyl radical react with C-11 at a diffusion controlled rate of $\sim 10^9\ M^{-1}\ s^{-1}$, faster than those of the alkoxyl radical RO· ($9{\cdot}10^6\ M^{-1}\ s^{-1}$) and peroxyl radical ROO· ($6{\cdot}10^1\ M^{-1}\ s^{-1}$) (Yin et al., 2011). Results of FLASH and CONV irradiations are presented in Fig. 2. CONV resulted in a dose-dependent increase in the lipid peroxidation yield as indicated by increased MDA levels with dose. Conversely,

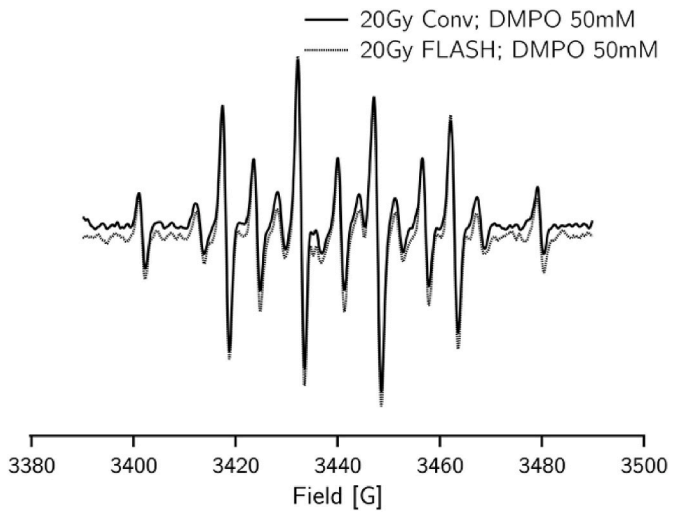

Fig. 1. ESR spectrum of HO· and H· spin trapping by 50 mM DMPO after Conv-RT (full line) and FLASH-RT (dotted line) at 20 Gy.

FLASH did not induce any lipid peroxidation, neither in linoleic acid micelles nor in phosphatidylcholine liposomes (Fig. 2a and b). Lowering the oxygen partial pressure from 21% atm down to physiologically relevant value of 4% atm of O_2 decreased lipid peroxidation levels after CONV but did not fully suppress it (Fig. 2c and d). Concentrations of MDA and LOOH measured after CONV at 4% O_2 tension were roughly halved in comparison to those registered at 21% O_2. In all our experiments, FLASH did not lead to significant formation of MDA and LOOH, either at 21 or 4% atm of O_2. This confirms that CONV-RT elicits robust lipid peroxidation, even at low O_2 concentration, whereas FLASH-RT does not.

To investigate further lipid peroxidation during irradiation, we carried out an experiment with the PC target (2 ml Eppendorf tube) placed at different depths in the water tank, recording the penetration of the beam in a tissue equivalent thickness. The percentage of depth dose (PDD) was estimated with an ionization chamber, which measured the absorbed dose to water at different depths (Fig. 3a).

Results showed that the lipid peroxidation yield decreases as a function of depth for CONV while FLASH was once again unable to induce significant lipid peroxidation (Fig. 3a). The comparison of the lipid peroxidation yield with the PDD revealed that the general behavior is similar, with a decrease as a function of depth. However, the PDD build-up region is not reproduced by the peroxidation curve and the decrease in MDA concentration occurs faster than the decrease in the PDD. Both observations are most likely a consequence of two effects: 1) the variation in the dose per pulse with depth; as shown in Fig. 3b, the peroxidation yield strongly depends on the dose per pulse. 2) The inner diameter of the 2 ml Eppendorf tube is 8 mm, causing significant dose variation across the sample; the measured MDA concentration at each depth corresponds to the average dose deposited to the sample at that depth. Also, the energy spectrum of electron beam changes with depth as well, which might have an effect on the peroxidation yield. Finally, considering all the aforementioned effects, the peroxidation yield seems to follow the electron fluence in the medium quite well, confirming once again its linearity with the dose in CONV mode. The aforementioned effects are all convoluted and it remains difficult to separate them with this sole experiment.

3.3. *Lipid peroxidation as a function of dose per pulse*

Our foregoing results demonstrated that CONV initiated lipid peroxidation while FLASH does not. Since one of the main electron beam parameters distinguishing FLASH from CONV is the dose per pulse, we investigated the dependency of the lipid peroxidation by varying the dose per pulse. Stark (1991) reviewed the effects of ionizing radiation on lipid membrane. The most striking result was the observation of the "inverse dose rate effect" which resulted in more damage observed at lower dose rate. Theoretical calculations showed that the high radical initiation rate, Ri, in high dose rate was responsible of more radical-radical recombinations, leading to shorter reaction chain length. Similarly, our results showed a rapid decrease in the MDA and LOOH concentrations (absorbance at 560 nm of the Fe^{3+}-XO complex) as a function of the dose per pulse, at a frequency of 10 Hz and pulse width of 1 μs (Fig. 3b). At a dose per pulse of 0.05 Gy·pulse^{-1}, the lipid peroxidation yield had already decreased by half compared to the lowest dose per pulse used of 0.008 Gy·pulse^{-1}. No apparent threshold was evident

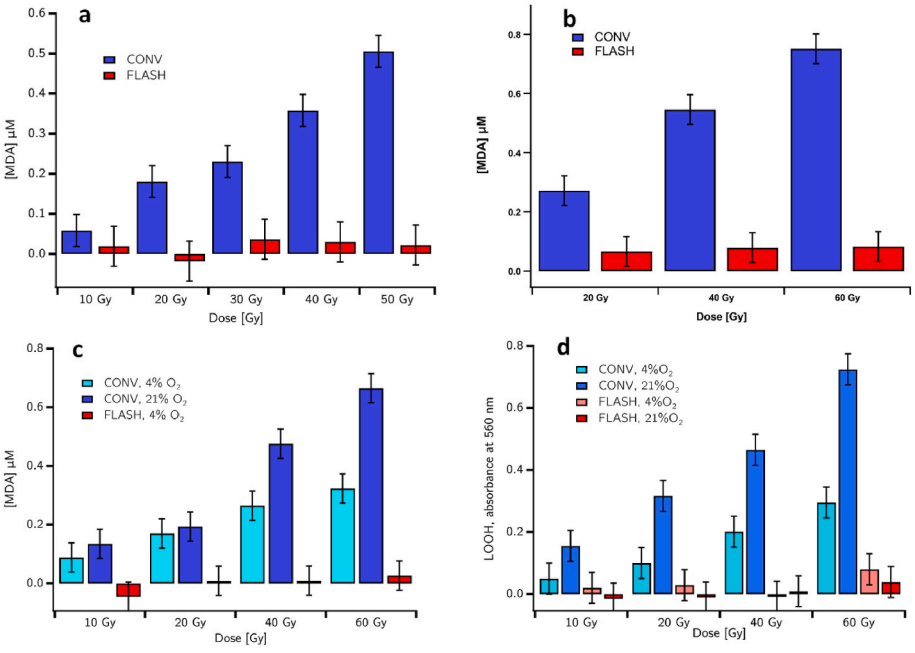

Fig. 2. MDA concentration [μM] after CONV-RT (blue) or FLASH-RT (red)
a) Linoleic acid micelles: 13 mM linoleic acid in 0.3% SDS buffered at pH 7.4 by 5 mM KH_2PO_4. **b)** PC liposomes: 5 mM phosphatidylcholine in 5 mM KH_2PO_4 buffered at pH 7.4. **c)** PC liposomes at 4% O_2 (light blue) and 21% O_2 (dark blue). LOOH absorbance after CONV-RT (blue) or FLASH-RT (red): **d)** Linoleic acid micelles 13 mM in 0.3% SDS buffered at pH 7.4 by 5 mM KH_2PO_4: LOOH (absorbance of Fe^{3+}-XO at 560 nm) at 4% O_2 (light blue) and 21% O_2 (dark blue) in Conv-RT and at 4% O_2 (pink) and 21% O_2 (red) in FLASH-RT.

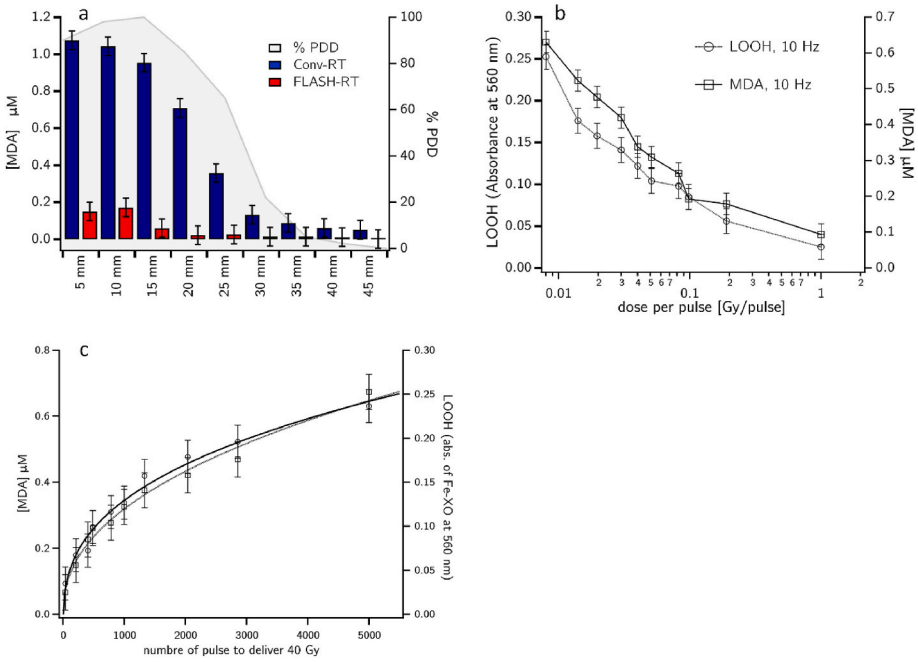

Fig. 3. Lipid peroxidation measured as [MDA] or [LOOH] absorbance signal as a function of the beam penetration depth and dose per pulse or number of pulses after FLASH and CONV irradiation.
a) MDA concentrations [µM] as a function of the distance from the water tank entry for CONV-RT (blue) and FLASH-RT (red) and comparison with the percentage of dose depth (light gray) measured by an ionization chamber; [PC] = 5 mM; [LA] = 2 mM in 5 mM KH_2PO_4 buffer at pH 7.4, dose = 30 Gy at 5 mm depth. **b)** MDA concentrations [µM, black line] and LOOH (absorbance at 560 nm of Fe^{3+}-XO, gray line) after irradiation of PC liposomes with embedded LA at various dose per pulse [Gy·pulse^{-1}] at a frequency of 10 Hz and a dose of 40 Gy. **c)** MDA concentrations [µM] as a function of the number of pulses to deliver 40 Gy [PC] = 5.2 mM, [LA] = 2 mM, in KH_2PO_4 5 mM at pH 7.4.

at high dose per pulse, but starting from a dose per pulse of 0.2 Gy·pulse^{-1}, levels of MDA and LOOH were very low or not detectable. We also did not observe any saturation of the increase in the MDA concentration down to the lowest dose per pulse achievable in our experimental setup. When expressed as a function of the number of pulses to deliver an isodose of 40 Gy, results for both MDA and LOOH showed that a small number of pulses resulted in low MDA and LOOH concentrations, while increasing the number of pulses resulted in a steady increase of both (Fig. 3c). Taking ε = 51,200 M^{-1} cm^{-1} as the extinction coefficient for the determination of the LOOH concentration by the Fe^{3+}-XO method, as determined by Gay and Gebicki (2003), the LOOH concentration at 0.008 Gy·pulse^{-1} was about 5.0 µM, roughly ten times higher than the MDA concentration. Both concentrations showed a similar pattern, indicating that LOO· (peroxyl radical) was the precursor of MDA, as MDA is formed by the cleavage of cyclic hydroperoxides. Because the formation of 1 mol of MDA requires the consumption of at least 10–20 mol of O_2 (Wills, 1969), the majority of the lipid peroxidation product was the lipid hydroperoxide, with lower amounts of other carbonyl compounds, such as 4-hydroxy-nonenal (not measured).

4. Discussion

This study is the first to measure lipid peroxidation after exposure of lipid micelles and PC liposomes mimicking cell membrane to various dose rate of irradiation and especially with FLASH-RT irradiation parameters. The most striking result of this work is a linear dose-response after CONV-RT, while FLASH-RT does not induce lipid peroxidation. Interestingly, lipid peroxidation occurred above 0.2 Gy·pulse-1 at 10 Hz, suggesting that the dose in the pulse is the relevant physical parameter to induce lipid peroxidation. Most importantly, our study shows that increasing the dose per pulse resulted in the inability to induce lipid peroxidation above 0.2 Gy·pulse^{-1} at 10 Hz. The value found in this chemical systems (0.2 Gy. pulse^{-1}) is however different from the value found in mice experiments where the neuroprotective effect of FLASH was lost below 1 Gy pulse^{-1} at 100 Hz (Montay-Gruel et al., 2017). This suggests that lipid peroxidation is not the only contributing factor to the FLASH effect in biological systems and that the pulse frequency might have a significant importance in the FLASH effect. Beside beam parameters, another important factor to understand the FLASH effect is the O_2 tension in the microenvironment. The oxygen enhancement ratio has been well described after irradiation at conventional dose rate and here with CONV irradiation, a dose-dependent increase in lipid peroxidation was measured, even at physiological O_2 concentration; a strong dose per pulse response, with a sharp decrease in peroxidation yield from 0.008 Gy·pulse^{-1} to 0.1 Gy·pulse^{-1} has been determined. Kusomoto et al. (Kusumoto et al., 2020) investigated the oxidation of the coumarin-3-carboxylic acid to fluorescent 7-hydroxy-coumarin-3-carboxylic acid after 27.5 MeV proton irradiation at various dose rate ranging from 0.05 to 160 Gy s^{-1}. Similar to our work, they observed a linear dependency of the coumarin-3-carboxylic acid oxidation concentration as a function of the absorbed dose and a steady decrease with increasing dose rate. They concluded that the basis of the FLASH effect is multifactorial, and involves a delicate balance between dose, oxygen availability and reactions induced by radicals, but mostly by oxygen depletion. Clearly, dose rate and oxygen depletion were not independent parameters and both influenced the coumarin oxidation yield. However, in their experiments, the coumarin-3-carboxylic acid was dissolved in water, with direct contact of the scavenging molecules with the water radiolysis radicals. In our case, the ROS diffuse to the linoleic acid micelles or the PUFA moieties in the PC liposomes, increasing the probability of radical recombination before reaching the target site (e.g. C-11 of LA). Thus, from a chemical point of view, diffusion of the hydroxyl radical to the target molecule (e.g. coumarin-3-carboxylic or linoleic acid or phospholipids) in a bi-molecular oxidation reaction is strictly dependent on the dose rate. This was confirmed in our case by a similar hydroxyl radical yield at 20 Gy for FLASH and CONV, as evidenced by the DMPO spin-trapping experiment (Fig. 1).

5. Conclusions

The lack of lipid peroxidation in FLASH compared to CONV-irradiated PC liposomes could be highly significant at the biological level and warrants further investigation. In this respect, FLASH-RT could balance the level of ferroptosis induced by irradiation. However, the differential impact of low lipid peroxidation level on tumors versus normal tissue after FLASH-RT is unclear, as one would expect that it should protect either healthy tissues and tumors or none of them. The idea that GPx4 *versus* ferroptosis balance could drive normal tissue

response to FLASH-RT is supported by the recent work of Chen et al., (2022) in a mouse model of Alzheimer's disease. However, ferroptosis agonists are described to be potent radiosensitizers after exposure to CONV-RT in tumors, whereas ferroptosis antagonists limit radiotherapy efficacy in tumor models (Lang et al., 2019). One can hypothesize that normal cells could be non-sensitive to the low level of lipid peroxidation by FLASH-RT whereas tumor cells could be highly sensitive to lipid peroxidation due to their altered redox-active iron metabolism, increased labile iron pool (Schoenfeld et al., 2017) and acidic pH milieu generated by the glycolytic shift and high level of lactate production (Hayes et al., 2020). This higher pool of labile iron would increase the reaction rate of Fenton chemistry to exacerbate tumor killing. Interestingly, both an increase in free iron concentration and low pH are hallmarks of a high lipid peroxidation yield. The iron and pH dependency could make cancer cells more vulnerable to iron-catalyzed ferroptosis following irradiation. To resolve these issues, work in our laboratory continues to investigate if/how FLASH is able to initiate significant lipid peroxidation in phosphatidylcholine liposomes under conditions of low pH and increased labile iron. These studies along with more complex chemical surrogates of the cellular milieu will be required to transfer these fundamental discoveries at the radiochemical level to the additional biologically relevant mechanisms able to account for the *in vivo* FLASH effect.

Funding

This work was funded by FNS Synergia grant MAGIC- FNS CRSII5_186369.

Author contributions

P.F. conceptualized and designed the study, carried out the measures and wrote most of the paper. V.G. carried out the irradiation and wrote part of the paper. C.B. designed and carried out the metrology of UHDR irradiation and wrote part of the manuscript. W.R.G. carried out the irradiation and wrote part of the paper. F.B. obtained funding and reviewed the manuscript M.C.V. designed part of the study, obtained funding and wrote part of the manuscript. All authors have read and approved the last version of the manuscript.

Declaration of competing interest

The authors declare that they have no known competing financial interests or personal relationships that could have appeared to influence the work reported in this paper.

Data availability

Data will be made available on request.

Acknowledgments

Laura Pfefferlé and Alexy Bonnin are thanked for their help in MDA measurements. Charles Limoli and Jean-François Germond are acknowledged for critical reading of the manuscript.

References

Abolfath, R., Grosshans, D., Mohan, R., 2020. Oxygen depletion in FLASH ultra-high-dose-rate radiotherapy: a molecular dynamics simulation. Med. Phys. 47 (12), 6551–6561.

Bourhis, J., Montay-Gruel, P., Jorge, P.G., Bailat, C., Petit, B., Ollivier, J., et al., 2019. Clinical translation of FLASH radiotherapy: why and how? Radiother. Oncol. 139, 11–17.

Buonanno, M., Grilj, V., Brenner, D.J., 2019. Biological effects in normal cells exposed to FLASH dose rate protons. Radiother. Oncol. 139, 51–55.

Chen, L.J., Dar, N.J., Na, R., McLane, K.D., Yoo, K.S., Han, X.L., et al., 2022. Enhanced defense against ferroptosis ameliorates cognitive impairment and reduces neurodegeneration in 5xFAD mice. Free Radic. Biol. Med. 180, 1–12.

Dixon, S.J., Stockwell, B.R., 2019. The hallmarks of ferroptosis. Annu. Rev. Cell Biol. 3, 35–54.

Doll, S., Proneth, B., Tyurina, Y.Y., Panzilius, E., Kobayashi, S., Ingold, I., et al., 2017. ACSL4 dictates ferroptosis sensitivity by shaping cellular lipid composition. Nat. Chem. Biol. 13, 91–98.

Favaudon, V., Caplier, L., Monceau, V., Pouzoulet, F., Sayarath, M., Fouillade, C., et al., 2014. Ultrahigh dose-rate FLASH irradiation increases the differential response between normal and tumor tissue in mice. Sci. Transl. Med. 6, 245ra93.

Fouillade, C., Curras-Alonso, S., Giuranno, L., Quelennec, E., Heinrich, S., Bonnet-Boissinot, S., et al., 2020. FLASH irradiation spares lung progenitor cells and limits the incidence of radio-induced senescence. Clin. Cancer Res. 26 (6), 1497–1506.

Gay, C.A., Gebicki, J.A., 2003. Measurement of protein and lipid hydroperoxides in biological systems by the ferric-xylenol orange method. Anal. Biochem. 315 (1), 29–35.

Hayes, J.D., Dinkova-Kostova, A.T., Tew, K.D., 2020. Oxidative stress in cancer. Cancer Cell 38 (2), 167–197.

Hendry, J.H., Moore, J.V., Hodgson, B.W., Keene, J.P., 1982. The constant low oxygen concentration in all the target-cells for mouse tail radionecrosis. Radiat. Res. 92 (1), 172–181.

Jaccard, M., Petersson, K., Buchillier, T., Germond, J.F., Duran, M.T., Vozenin, M.C., et al., 2017. High dose-per-pulse electron beam dosimetry: usability and dose-rate independence of EBT3 Gafchromic films. Med. Phys. 44, 725–735.

Jaccard, M., Duran, M.T., Petersson, K., Germond, J.F., Liger, P., Vozenin, M.C., et al., 2018. High dose-per-pulse electron beam dosimetry: commissioning of the Oriatron eRT6 prototype linear accelerator for preclinical use. Med. Phys. 45, 863–874.

Jorge, P.G., Grilj, V., Bourhis, J., Vozenin, M.C., Germond, J.F., Bochud, F., et al., 2022. Validation of an ultrahigh dose rate pulsed electron beam monitoring system using a current transformer for FLASH preclinical studies. Med. Phys. 49, 1831–1838.

Kacem, H., Almeida, A., Cherbuin, N., Vozenin, M.C., 2021. Understanding the FLASH effect to unravel the potential of ultra-high dose rate irradiation. Int. J. Radiat. Biol. 98 (3), 506–516.

Kusumoto, T., Kitamura, H., Hojo, S., Konishi, T., Kodaira, S., 2020. Significant changes in yields of 7-hydroxy-coumarin-3-carboxylic acid produced under FLASH radiotherapy conditions. RSC Adv. 10 (63), 38709–38714.

Labarbe, R., Hotoiu, L., Barbier, J., Favaudon, V., 2020. A physicochemical model of reaction kinetics supports peroxyl radical recombination as the main determinant of the FLASH effect. Radiother. Oncol. 153, 303–310.

Lang, X.T., Green, M.D., Wang, W.M., Yu, J.L., Choi, J.E., Jiang, L., et al., 2019. Radiotherapy and immunotherapy promote tumoral lipid oxidation and ferroptosis via synergistic repression of SLC7A11. Cancer Discov. 9, 1673–1685.

Lei, G., Zhang, Y.L., Koppula, P., Liu, X.G., Zhang, J., Lin, S.H., et al., 2020. The role of ferroptosis in ionizing radiation-induced cell death and tumor suppression. Cell Res. 30, 146–162.

Lei, G., Mao, C., Yan, Y.L., Zhuang, L., Gan, B.Y., 2021a. Ferroptosis, radiotherapy, and combination therapeutic strategies. Protein Cell 12, 836–857.

Lei, G., Zhang, Y.L., Hong, T., Zhang, X.D., Liu, X.G., Mao, C., et al., 2021b. Ferroptosis as a mechanism to mediate p53 function in tumor radiosensitivity. Oncogene 40, 3533–3547.

Mead, J.F., 1952. The irradiation-induced autoxidation of linoleic acid. Science 115 (2991), 470–472. https://doi.org/10.1126/science.115.2991.470.

Montay-Gruel, P., Petersson, K., Jaccard, M., Boivin, G., Germond, J.F., Petit, B., et al., 2017. Irradiation in a flash: unique sparing of memory in mice after whole brain irradiation with dose rates above 100 Gy/s. Radiother. Oncol. 124, 365–369.

Montay-Gruel, P., Acharya, M.M., Petersson, K., Alikhani, L., Yakkala, C., Allen, B.D., et al., 2019. Long-term neurocognitive benefits of FLASH radiotherapy driven by reduced reactive oxygen species. P. Nat.Acad. Sci. USA 116 (22), 10943–10951.

Montay-Gruel, P., Acharya, M.M., Jorge, P.G., Petit, B., Petridis, I.G., Fuchs, P., Leavitt, et al., 2021. Hypofractionated FLASH-RT as an effective treatment against glioblastoma that reduces neurocognitive side effects in mice. Clin. Cancer Res. 27 (3), 775–784.

Oesterle, R., Jorge, P.G., Grilj, V., Bourhis, J., Vozenin, M.C., Germond, J.F., et al., 2021. Implementation and validation of a beam-current transformer on a medical pulsed electron beam LINAC for FLASH-RT beam monitoring. J. Appl. Clin. Med. Phys. 22, 165–171.

Pearson, A.N., Carmicheal, J., Jiang, L., Lei, Y.L., Green, M.D., 2021. Contribution of lipid oxidation and ferroptosis to radiotherapy efficacy. Int. J. Mol. Sci. 22, 12603.

Petersson, K., Jaccard, M., Germond, J.F., Buchillier, T., Bochud, F., Bourhis, J., et al., 2017. High dose-per-pulse electron beam dosimetry - a model to correct for the ion recombination in the Advanced Markus ionization chamber. Med. Phys. 44, 1157–1167.

Schoenfeld, J.D., Sibenaller, Z.A., Mapuskar, K.A., Wagner, B.A., Cramer-Morales, K.L., Furqan, M., et al., 2017. O_2 and H_2O_2-mediated disruption of Fe metabolism causes the differential susceptibility of NSCLC and GBM cancer cells to pharmacological ascorbate. Cancer Cell 31, 487–500.

Simmons, D.A., Lartey, F.M., Schuler, E., Rafat, M., King, G., Kim, A., et al., 2019. Reduced cognitive deficits after FLASH irradiation of whole mouse brain are associated with less hippocampal dendritic spine loss and neuroinflammation. Radiother. Oncol. 139, 4–10.

Spitz, D.R., Buettner, G.R., Petronek, M.S., St-Aubin, J.J., Flynn, R.T., Waldron, T.J., et al., 2019. An integrated physico-chemical approach for explaining the differential impact of FLASH versus conventional dose rate irradiation on cancer and normal tissue responses. Radiother. Oncol. 139, 23–27.

Stark, G., 1991. The effect of ionizing radiation on lipid membranes. Biochim. Biophys. Acta 1071 (103), 122.
Stockwell, B.R., Angeli, J.P.F., Bayir, H., Bush, A.I., Conrad, M., Dixon, S.J., et al., 2017. Ferroptosis: a regulated cell death nexus linking metabolism, redox biology, and disease. Cell 171, 273–285.
Vozenin, M.C., Hendry, J.H., Limoli, C.L., 2019. Biological benefits of ultra-high dose rate FLASH radiotherapy: sleeping beauty awoken. Clin. Oncol. 31 (7), 407–415.
Weiss, H., Epp, E.R., Heslin, J.M., Ling, C.C., Santomasso, A., 1974. Oxygen depletion in cells irradiated at ultrahigh dose-rates and conventional dose-rates. Int. J. Radiat. Biol. 26 (1), 17–29.
Wiernicki, B., Dubois, H., Tyurina, Y.Y., Hassannia, B., Bayir, H., Kagan, V.E., et al., 2020. Excessive phospholipid peroxidation distinguishes ferroptosis from other cell death modes including pyroptosis. Cell Death Dis. 11, 922.
Wills, E.D., 1969. Lipid peroxide formation in microsomes-general considerations. Biochem. J. 113 (2), 315–324.
Yin, H.Y., Xu, L.B., Porter, N.A., 2011. Free radical lipid peroxidation: mechanisms and analysis. Chem. Rev. 111 (10), 5944–5972.
Zhang, W.N., He, H.B., Feng, Y.Q., Da, S.L., 2003. Separation and purification of phosphatidylcholine and phosphatidylethanolamine from soybean degummed oil residues by using solvent extraction and column chromatography. J. Chromatogr. B 798 (2), 323–331.